FISSION OF METALLIC CLUSTERS

CARLOS FIOLHAIS

and

ARMANDO VIEIRA

Center for Theoretical Physics, University of Coimbra, 3000 Coimbra, Portugal

ABSTRACT

The fission of sodium clusters is discussed using Nuclear Physics methods. After presenting the Liquid Drop Model for spherical jellium clusters, we introduce shell corrections and compare the obtained energies with self-consistent quantal results. Fission is studied evaluating Q-values and fission barriers, with the shell correction method and the Two Center Shell Model. The threshold of stability with respect to fission is predicted within the Liquid Drop Model.

1. Introduction

Metallic clusters are many-body systems which show striking similarities with atomic nuclei: the valence electrons move in a mean-field as nucleons move in the nuclear mean-field. An important difference is that a part of the mean-field is externally imposed (by the ions) while the whole nuclear mean-field is self-organized by the participants.

Metallic clusters were produced by the middle of the eighties. The static mean field was experimentally identified by a group led by Knight [1]. At the same time but independently, Ekardt [2] predicted the existence of independent particle motion for the valence electrons.

The success in analyzing clusters in the laboratory is due mainly to progresses achieved in the technology of molecular beams. A typical setup consists of a chamber where a metallic sample is vaporized with the aid of a laser. The atoms which are set free may coalesce in clusters, which are transported by a high speed helium beam through an exit channel. The molecular beam is directed to a mass spectrometer. A second laser ionizes the clusters so that they are deviated by a magnetic field and sorted according to its size.

A clear sign for the mean field is the appearance of the magic numbers 8, 20, 40, 58, etc. as peaks in the relative abondances in the mass spectrometer. Another indication comes from the ionization potential, which also shows peaks for clusters with 8, 20, 40, 58, etc. valence electrons. The first two of these magic numers are the same as in atomic nuclei, but the others differ. In fact, the nuclear magic numbers can be well described by a strong spin-orbit splitting, a relativistic effect which is negligicible for clusters. Therefore, a simple Woods-Saxon shape of the mean field, or even a simpler harmonic oscillator for the lightest systems, can explain the correct shell closures in clusters. We can talk about the ubiquity of the shell model, which dominates the structure of atoms, metallic clusters, and nuclei, notwithstanding the fact that there are six orders of magnitude in energy difference between the atomic

and the nuclear domains.

We emphasize that the magic effects in metallic particles arise from the confinement of the electrons and not from the geometrical arrangements of the ions. The physical properties for sp-metals (the only ones which we consider here) are due to the weakly bonded valence electrons and not to the inert cores, which only provide the space where the valence electrons are delocalized. It is difficult to ascertain experimentally (and even theoretically, due to the large number of isomers which differ little in energy) the geometrical disposition of the ions. But it evolves gradually from planar shapes, typical of clusters with up to 4 atoms, to close packed structures. The minimal number of atoms which are necessary to form a piece of material with a given bulk property seems to depend on the particular material and on the particular property.

Clusters are intermediate structures between the atoms and bulk matter in the same way as nuclei are intermediate structures between one nucleon and nuclear matter, which exists in neutron stars. One of the main motivations for studying clusters is precisely the possibility of filling a bridge between the properties of individual atoms and molecules and normal macroscopic matter. In Nuclear Physics, the increase of Coulomb repulsion with the atomic number determines a maximal size for the nuclides. The heavier nuclei decay by spontaneous fission or alpha emission. In spite of that repulsion, one has speculated about the existence of big magic numbers which would give rise to one or more islands of "superheavy nuclei". Cluster physics offers the opportunity to look for similar magic numbers, in large atomic systems, where Coulomb instability is not present.

The theoretical analysis of clusters requires techniques from Solid State Physics as well as from Quantum Chemistry, being Cluster Physics a field where cross fertilization of different methodologies is taking place. Given the analogies between clusters and nuclei, it is natural that concepts and tools from Nuclear Physics disseminate in the new research area. We intend to present here some examples.

In the next section, we sketch the theoretical framework for our approach to clusters, neutral as well as charged. The case is presented for the "import" of the Liquid Drop Model (LDM) and the shell correction method from Nuclear Physics and the possible "export" to Nuclear Physics of some information on the curvature energy of metallic clusters and voids. In section 3, we address the problem of the fission of metallic clusters, considering Q-values and barrier heights obtained with the aid of Kohn-Sham theory, LDM, and the shell correction method. Some general conclusions are drawn at the end.

2. Theoretical tools: self-consistent equations versus the shell-correction method

Density functional methods are very powerful tools in Atomic, Molecular and Condensed Matter Physics. For big enough systems they are the only accurate methods which are feasible.

They are based on an existence theorem due to Hohenberg and Kohn [3,4], according to which the ground-state energy of a many-electron system is a functional of the local electronic density $E = E[n(r)]$. Minimization of this functional with respect to the density would give the exact density and the exact energy if the functional were

known:

$$\frac{\delta E[n]}{\delta n} = 0. \tag{1}$$

The energy is separated in kinetic, electrostatic (Hartree term), exchange and correlation, and the contribution from a local external potential:

$$E[n] = T_s[n] + E_{es}[n] + E_{xc}[n] + \int v_{ext}\, n\, d^3\mathrm{r}. \tag{2}$$

The unknown part is the exchange and correlation piece, $E_{xc}[n]$, for which approximations like the Local Density Approximation (LDA) are mandatory.

A starting point for modelling the ions, which are the source of the external potential felt by the valence electrons, is the so-called jellium approximation [5,6]. The ions are replaced by an uniform distribution of positive charge. This approximation has proved to be useful in the study of bulk and surface properties of simple metals. In the jellium approximation, the electrons interact with the positive background and with themselves.

The radius R of the jellium sphere corresponding to a neutral cluster with N valence electrons goes with the cubic root of N simply due to the neutrality of the cluster:

$$R = r_s N^{\frac{1}{3}}, \tag{3}$$

where r_s is the so-called density parameter, which goes from 1.87 bohr for beryllium to 5.63 bohr for caesium. This is the radius of the sphere occupied by one valence electron. It corresponds in Nuclear Physics to the parameter $r_0 = 1.2$ fm. The density of positive charge is given by a step function:

$$n_+(r) = \overline{n}\,\theta(R - r), \tag{4}$$

with $\overline{n} = (3/4\pi r_s^3)^{-1}$ the average density. The jellium functional has an electrostatic piece which depends on both n and n_+ (including electron-jellium, electron-electron and jellium-jellium interactions):

$$\begin{aligned} E_{jell} &= T_s[n] + E_{es}[n, n_+] + E_{xc}[n], \\ E_{es}[n, n_+] &= \frac{1}{2}\int d^3\mathrm{r} \int d^3\mathrm{r}' \frac{[n(\mathrm{r}') - n_+(\mathrm{r}')]}{|\mathrm{r}' - \mathrm{r}|}[n(\mathrm{r}) - n_+(\mathrm{r})]. \end{aligned} \tag{5}$$

In the jellium model, the energy of a spherical cluster, as a function of N and r_s, can be evaluated solving Eq. (1), called Kohn-Sham equation, within the LDA approximation. That equation reads as (in atomic units):

$$\Big[-\frac{1}{2}\nabla^2 + v_{eff}(\mathrm{r})\Big]\psi_\alpha(\mathrm{r}) = \epsilon_\alpha \psi_\alpha(\mathrm{r}) \ , \tag{6}$$

where α denotes a set of quantum numbers. The effective potential is

$$v_{eff}(\mathrm{r}) = v_+(\mathrm{r}) + \int d^3\mathrm{r}' \frac{n(\mathrm{r}')}{|\mathrm{r} - \mathrm{r}'|} + \mu_{xc}(\mathrm{r}) \quad , \tag{7}$$

with the external (jellium) potential

$$v_+(\mathrm{r}) = \begin{cases} -\frac{N}{2R}\left[3 - \left(\frac{r}{R}\right)^2\right] & (r < R) \\ -\frac{N}{r} & (r > R) \end{cases} , \tag{8}$$

and $\mu_{xc}(r)$ the exchange-correlation potential,

$$\mu_{xc}(\mathrm{r}) = \frac{\delta}{\delta n(\mathrm{r})}\left[n(\mathrm{r})\epsilon_{xc}(\mathrm{r})\right] , \tag{9}$$

with $\epsilon_{xc} = -3k_F/4\pi + \epsilon_c$. The quantity $\epsilon_c = \epsilon_c(r_s)$ is the correlation energy per electron of the uniform electron gas and $k_F = (\frac{4\pi}{3})^{1/3}/r_s$ (we use the Perdew-Wang correlation energy [7]).

The total electronic density is

$$n(\mathrm{r}) = \sum_\alpha |\psi_\alpha(\mathrm{r})|^2 . \tag{10}$$

Once the self-consistent density has been obtained, the total energy is given by the functional:

$$E[n] = \sum_\alpha \epsilon_\alpha - \left[U[n] + \int d^3\mathrm{r}\ \mu_{xc}(\mathrm{r})n(\mathrm{r})\right] + U_B[n_+] + \int d^3\mathrm{r}\ \epsilon_{xc}(\mathrm{r})n(\mathrm{r}) , \tag{11}$$

where

$$U[n] = \frac{1}{2}\int d^3\mathrm{r} \int d^3\mathrm{r}' \frac{n(\mathrm{r})n(\mathrm{r}')}{|\mathrm{r} - \mathrm{r}'|} \tag{12}$$

is the electronic Coulomb repulsion energy and

$$U_B[n_+] = \frac{3}{5}\frac{N^2}{R} \tag{13}$$

is the background Coulomb repulsion.

Fig. 1 shows the results for the selfconsistent density for $N = 42$. We also show the net charge distribution for the double positively ionized system. We see that the excess charge lies mainly in the surface region. The electronic density profile is similar to the corresponding nuclear quantity: the density is constant inside (apart from shell fluctuations) and decreases to zero at the edge. Within our model of metallic clusters, the inner electronic density is determined by the jellium density: it is the same for different clusters of the same metal, but varies from metal to metal. In contrast, the nuclear density is constant for all nuclides, neglecting self-compression effects.

We may think that, given the parentage between nuclei and clusters, a liquid drop formula for the energy of electronic systems is accurate to describe average trends. The energy of a set of neutral clusters of the same element with different number of atoms can indeed be described by a sum of volume, surface and curvature terms. In

the case of charged systems, there is in addition an explicit contribution from the charge.

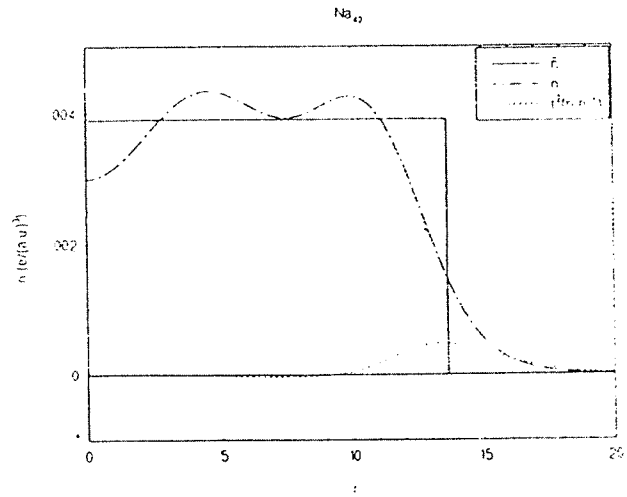

Figure 1: Jellium and valence electronic density $n(r)$ for Na_{42} obtained with the LDA Kohn-Sham method, in the jellium model. The dashed curve represents, in a different scale, the charge difference between the neutral and the double positively ionized system.

Contrary to some widespread belief, the liquid drop formula is not a phenomenological expression but can be derived from first principles with the aid of density functional methods. The energy of a spherical neutral cluster in the so-called leptodermeous expansion [8] (valid for systems with thin skin) can be written:

$$E[n] = E_{LDM} = \sum_{k=0}^{\infty} C_k R^{3-k} = \alpha \frac{4}{3}\pi R^3 + \sigma\, 4\pi R^2 + \gamma\, 2\pi R + \ldots \qquad (14)$$

The first term is the volume energy, the second is the surface energy, and the third is the curvature energy. The surface tension σ and the curvature energy γ are functionals of the electronic density of the semi-infinite problem [9].

The LDM coefficients obtained within the jellium model for the density of sodium, $r_s = 3.93$ bohr, are: $\alpha = -8.26 \times 10^{-3}$ eV/bohr^3, $\sigma = 2.96 \times 10^{-3}$ eV/bohr^2, and $\gamma = 9.97 \times 10^{-3}$ eV/bohr. The values of σ and γ were evaluated solving the semi-infinite problem (Lang-Kohn calculation [10]).

Let us now consider a spherical jellium cluster with N atoms and net charge Q. The liquid drop energy of this cluster, up to the order $N^{-\frac{1}{3}}$, is the sum of (14) with two charge contributions [11,12]:

$$E_{LDM} = \alpha V + \sigma S + \gamma C + Q(W + \frac{c}{R}) + \frac{1}{2}\frac{Q^2}{R + d_s}, \qquad (15)$$

where V is the cluster volume, S the surface and C the curvature. The quantity $-(W + \frac{c}{R})$ is the chemical potential, with W the work function and c a coefficient which describes a size effect (for sodium, $W = 2.85$ eV, and $c = -2.24$ eV [13]). The last term in Eq. (15) is the classical electrostatic energy, obtained under the assumption that the metal cluster is a perfect conductor and, therefore, the charge lies on the surface. A small spill-out effect due to the accumulation of excess charge on a radial centroid outside the jellium edge is included. The distance $R + d_s$ is the radius of the charge centroid (for sodium, $d_s = 1.1$ bohr).

From Fig. 2 we see that the LDM gives a good average of the Kohn-Sham energies of small spherical jellium clusters, neutral as well as charged. In order to ascertain the relative importance of the curvature energy, the insert shows the liquid drop result with and without the curvature term. We conclude that the curvature contribution plays a role only for very small clusters.

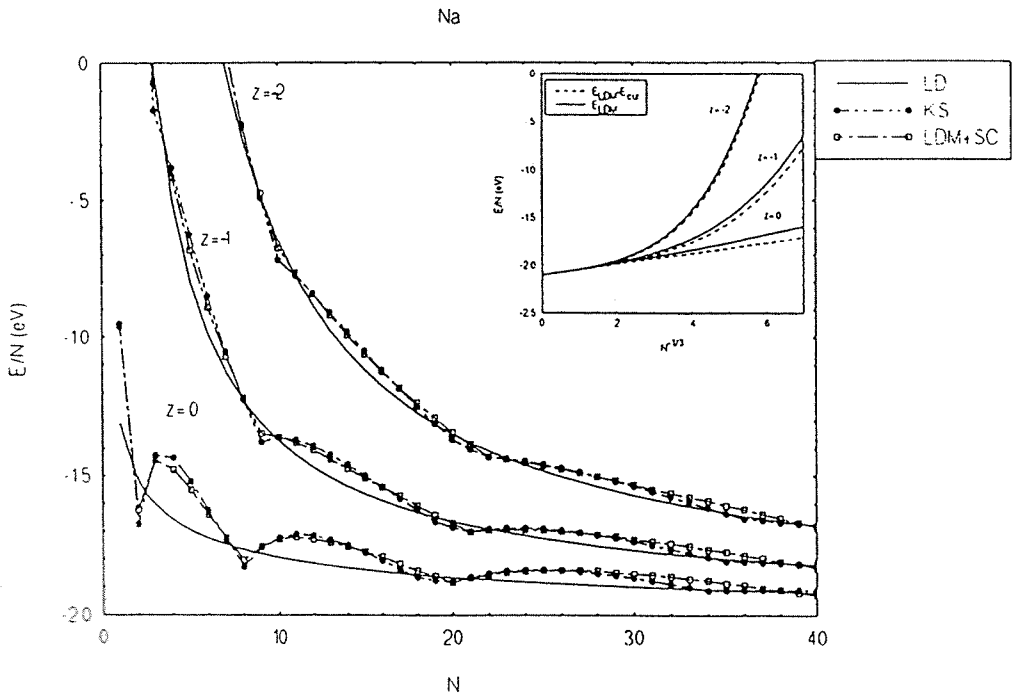

Figure 2: LDM and Strutinsky energies per atom of spherical jellium clusters of sodium, with $Q = 0, +1$ and $+2$ (the number of excess electrons is, respectively, $z = 0, -1$ and -2), in comparison with LDA Kohn-Sham results. In the insert, the LDM energy per atom, with and without the curvature term, is shown as a function of $N^{-\frac{1}{3}}$ for the same systems.

A system which provides a good test of the LDM is a spherical void inside jellium. Fig. 3 shows a comparison of the liquid drop formula with self-consistent calculations for the density $r_s = 2.07$ bohr. The agreement is excellent up to radii smaller than

a monoatomic void. The picture also shows a Padé approximant which has the right asymptotic behaviour for vanishing voids and coincides with the liquid drop formula for large voids [14,15]. A systematic comparison of LDM predictions with experimental void formation energies shows the role of curvature [16].

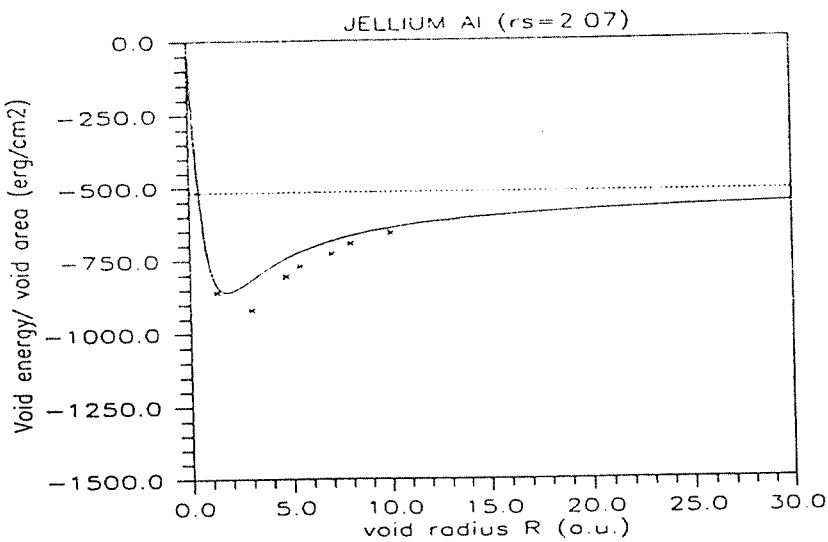

Figure 3: Void formation energies in the jellium model using the LDA Kohn-Sham method (crosses), the LDM (dotted line) and the Padé approximant of Ref. [15] (full line).

The von Weizaecker formula for the nuclear binding energy is well-known. Without the asymmetry term, it reads as

$$E_{LDM}(A,Z) = a_v A + a_s A^{\frac{2}{3}} + a_c A^{\frac{2}{3}} + a_{Coul}\frac{Z^2}{A^{\frac{1}{3}}}, \tag{16}$$

with the coefficients $a_v = -15.85$ MeV, $a_s = 18.34$ MeV, and $a_{Coul} = 0.71$ MeV, A being the mass number and Z the atomic number. There are various theoretical indications that the curvature coefficient is $a_c \simeq 10$ MeV. However, the experimental information on the nuclear binding energies is compatible with zero curvature energy. This is the so-called "curvature energy puzzle" in Nuclear Physics [17]. The success in Metal Physics of the leptodermous expansion is a strong suggestion that the value 10 MeV is right. However, if the leptodermous expansion does not converge quickly enough, higher order terms (which could be accounted for by a Padé formula) may be important and effectively cancel the curvature contribution.

In the Strutinsky shell correction method [18,19], the energy is given by the sum of a LDM term and a shell correction term,

$$E = E_{LDM} + E_{SC}, \tag{17}$$

where the last term may be evaluated as indicated in Ref. [20].

In order to check the validity of the shell correction method, we compare (17) with LDA Kohn-Sham calculations of spherical jellium clusters. Fig. 2 displays the very good agreement of the LDM plus shell corrected energies with the quantal ones. The shell structure is well reproduced with the simple harmonic oscillator up to $N = 42$. A small discrepancy occurs in the region around $N = 34$ (neutral case), where the $1f$ shell is being closed in the Kohn- Sham description, whereas that only happens for $N = 40$ in the case of the harmonic oscillator. We show results for the smallest clusters, keeping the same shell correction parameters, since, remarkably enough, they still compare rather well with the quantal energies.

3. Two Center Shell Model for the fission of charged jellium clusters

Small multiply charged clusters are not observed experimentally. This is due to the fact that charged atomic clusters with less than some critical number of atoms undergo fission, *i.e.*, fragmentation in two or more pieces with smaller charges [21,31]. The preferred decay channel of charged clusters above the critical size is the evaporation of neutral atoms: the heat of evaporation is lower than the fission barrier. In order to learn about cluster stability, it is convenient to have estimates as simple as possible of barrier heights and evaporation energies.

3.1. Quantal and LDM Q-values

An essential limitation on fission arises from the Q-values or heats of reaction, defined as the difference between final and initial energies. A positive heat of reaction means that the reaction can take place on pure energetic considerations but does not assure that the reaction is actually taking place (it is a necessary but not sufficient condition for fission). We consider both Kohn-Sham and LDM Q-values assuming always spherical configurations. Q-values obtained with the shell correction method agree, in general, with the self-consistent ones.

Figs. 4 (a) and (b) shows the Q-values, obtained with the Kohn-Sham method, corresponding to all possible decay channels of single and double positively charged sodium clusters up to $N = 30$. We only find Kohn-Sham solutions with total negative energies when $N > 2$ for single charged clusters and $N > 7$ for doubly charged clusters. The role of shell closures is apparent. Magic mother clusters, as for instance Na_{20}^{++}, are specially stable. On the other hand, final magic daughters, as for instance Na_3^+, are a common outcome.

The Q-values obtained with the LDM are shown in Figs. 4 (c) and (d) . For the single charged system, the asymmetric reaction $Na_N^+ \rightarrow Na_{N-1}^+ + Na_1$ is always preferred since it corresponds to a minimal Coulomb energy of the final configuration. This observation agrees with the Kohn-Sham results of Fig. 4 (a). In contrast, the symmetric channel $Na_N^{++} \rightarrow Na_{N/2}^+ + Na_{N/2}^+$ is preferred by doubly charged sodium clusters up to $N = 28$. A symmetric charge distribution of the fragments lowers indeed the total Coulomb energy for small clusters. This conclusion is not clearly seen in Fig. 4 (b), since shell effects play a major role for small clusters, hiding any smooth trend. However, a central valley is visible for $N > 20$.

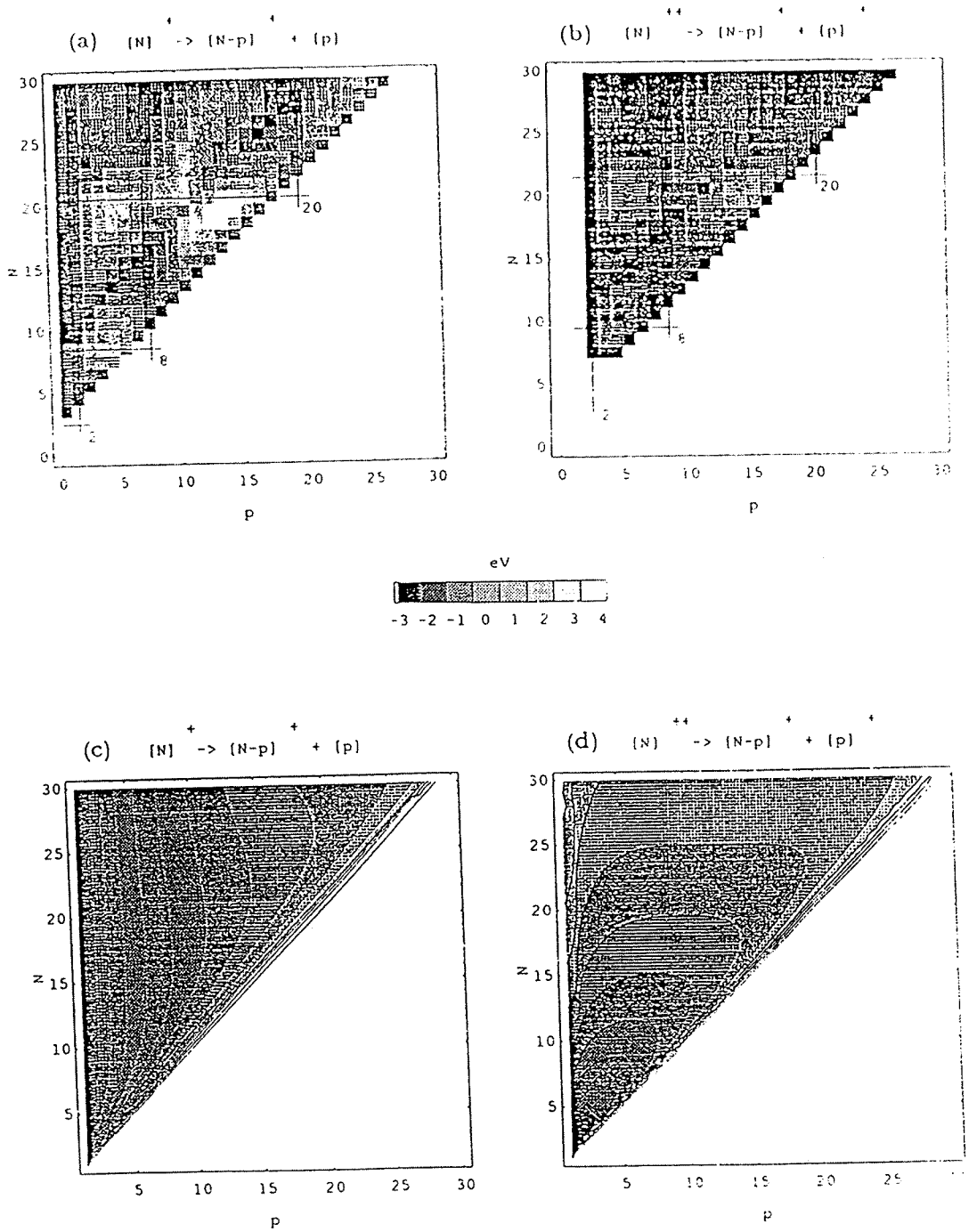

Figure 4: LDA Kohn-Sham Q-values for (a) Na_N^+ and (b) Na_N^{++} for every possible decay channel. Vertical and horizontal lines mark mothers and daughters with magic numbers of atoms. In (c) and (d) same as above but within the LDM.

Fig. 5 displays the Q-values for the most favorable channel obtained by using both the Kohn- Sham and the LDM approaches. We observe that the most favorable channel always has one magic fragment. This agrees with the results obtained in Ref. [22] (see also Ref. [23], which uses the "stabilized jellium model" for aluminium).

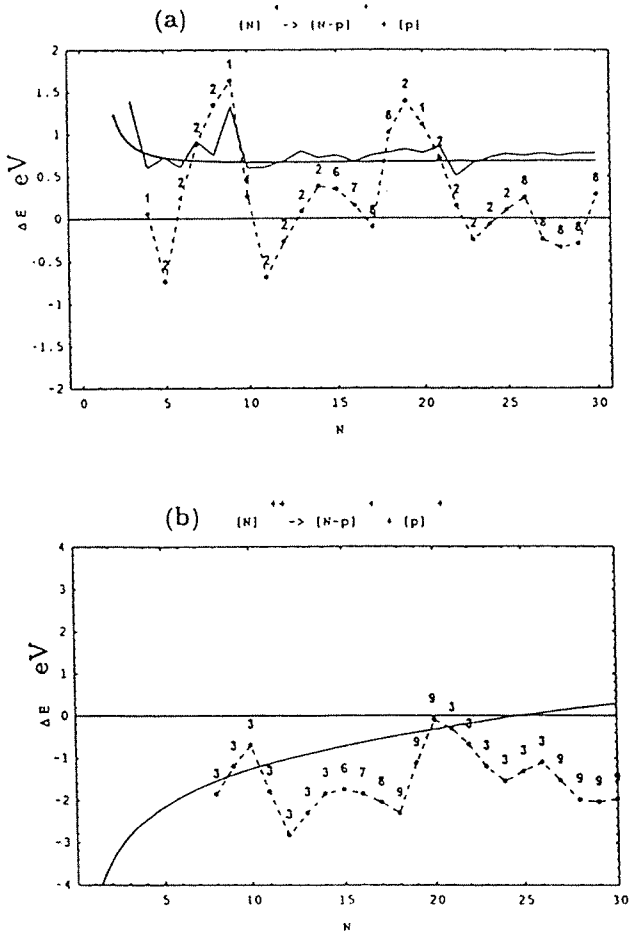

Figure 5: Q-values for the most favored decay channel for (a) Na_N^+ and (b) Na_N^{++}. The smooth line stands for the LDM, while the dots represent quantal results (the numbers above the dots are the values of p). In (a) the experimental results from Ref. [24] are represented by a thin broken line.

Fig. 5 (a) shows experimental results [24] obtained for single charged sodium clusters against our results. The agreement of the LDM with experiment is remarkable. The trends of the experimental results are also well reproduced by the quantal result, although fluctuations are exaggerated in the latter due the imposed sphericity.

In Fig. 5 (b) the two lowest local minima occurs when both fragments are magical: $Na_{12}^{++} \rightarrow Na_9^{+} + Na_3^{+}$ and $Na_{18}^{++} \rightarrow Na_9^{+} + Na_9^{+}$. As expected, the LDM curve goes slightly above the quantal results.

3.2. Deformed LDM and shell corrections

To evaluate the potential energy corresponding to the fission of sodium clusters, using the shell correction method, we need to generalize the LDM to handle deformed systems and to consider a shell model which can describe splitted shapes [25].

We have calculated potential energies for charged clusters which fragment in two pieces, in the framework of the LDM plus shell corrections obtained from the Two Center Shell Model, a double harmonic well which is popular in Nuclear Physics [26,27].

Eq. (17) may be extended to account for deformed clusters with the same volume as a spherical cluster:

$$E_{LDM} = \alpha V + \sigma S + \gamma C + Q(W' + \frac{c}{C/2\pi}) + a_{Coul}Q^2, \tag{18}$$

where the surface $S = \int dA$ of the deformed shape and $C = \frac{1}{4}\int \mathcal{R}^{-1} dA$, with $\mathcal{R}$ the local curvature, are evaluated numerically. In the size correction to the chemical potential $C/2\pi$ has replaced R, since this gives the right behaviour for one initial and two final spherical clusters.

The electrostatic energy of a spherical shell is now $a_{Coul}Q^2$, with the coefficient a_{Coul} computed numerically. This is done by minimizing the electrostatic energy under the constraint that the electric potential is constant on the cluster surface [28]. The spill-out effect is included by considering a surface charge which is displaced by d_s with respect to the shape with volume V.

As a set of shapes going from one sphere to two spheres, we select the so-called Blocki's shapes [29], which consists basically of two spheres joined by a smooth neck. This family is described by three parameters: an elongation parameter, a neck parameter and an asymmetry parameter, defined respectively by:

$$\rho = \frac{d}{R_1 + R_2}, \quad \lambda = \frac{l_1 + l_2}{R_1 + R_2}, \quad \Delta = \frac{R_1 - R_2}{R_1 + R_2}, \tag{19}$$

where d is the center to center distance, R_1 and R_2 are the radii of the two fragments, and l_1 and l_2 are the thickness of the lens-shaped piece of the sphere that lies within the matching quadratic surface.

For the path in the (ρ, λ) plane, we assume, based on molecular dynamics results [30], that initially the system does not develop a neck, getting it very quickly in the later stages of fission. Within the liquid drop picture, the energy along the fission line (curve which separates connected from disconnected shapes, given by the equation $\lambda = 1 - 1/\rho$) has a minimum at a saddle point. For obtaining fission barriers, the precise path is unimportant provided it goes through the saddle point.

We are interested not only in evaluating fission barriers but also in comparing them with evaporation energies. We consider the symmetric fragmentation of Na_{18}^{++} and Na_{42}^{++}, for which the final configurations are magic.

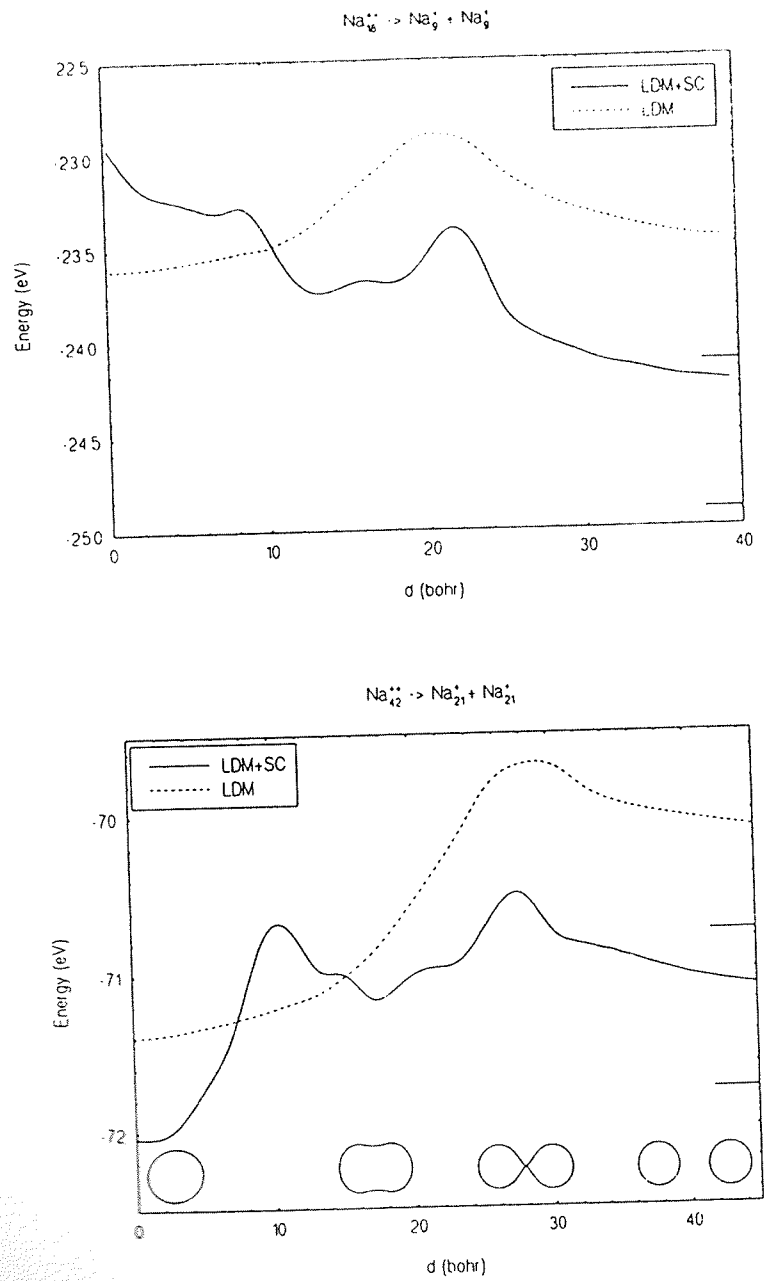

Figure 6: Potential energies for two fission processes using both the LDM and the LDM plus shellcorrections.

Fig. 6 show the potential energy curves for the two reactions along the path described in Ref. [25]. In the case of Na_{18}^{++}, the system shows a well deformed ground state and a small barrier at $d = 20$ bohr, being clearly unstable. In the case of Na_{42}^{++}, the system shows an initial spherical state and a fission isomer at $d = 16$ bohr.

The following Table informs about Q-values, heats of evaporation and fission barriers for the symmetric decays of Na_{18}^{++} and Na_{42}^{++}:

Table: Q-values and heats of evaporation E_{eva}, in the Kohn-Sham method (in brackets the corresponding values using the Strutinsky method). The fission barrier E_b given by the Strutinsky method is also shown. All values are in eV.

Reaction	Q-value	E_{eva}	E_b
$Na_{18}^{++} \rightarrow 2Na_8^+$	-2.05	2.13	
	(-2.06)	(2.19)	(0.53)
$Na_{42}^{++} \rightarrow 2Na_{21}^+$	0.25	1.28	
	(-0.45)	(1.10)	(1.62)

The agreement between the Kohn-Sham and the Strutinsky results is good. The discrepancy for the heat of reaction of Na_{42}^{++} is due to the failure of the harmonic shell correction for clusters around $N = 40$. We note that Na_{42}^{++} can decay symmetricaly on the basis of the Q-value if we calculate it *a la* Kohn-Sham, but the double humped barrier represents a serious hindering of fission. For this system, evaporation is preferred to fission, since $E_{eva} < E_b$.

Finally, we present a LDM estimate of the cluster size, N_c, for which $E_{eva} = E_b$ in the case of doubly charged sodium clusters. We do not make any restrictions on the size of the fission fragments, but for simplicity neglect the curvature term contribution to the barrier. In Fig. 7 we plot the fission barrier height for the most favored channel

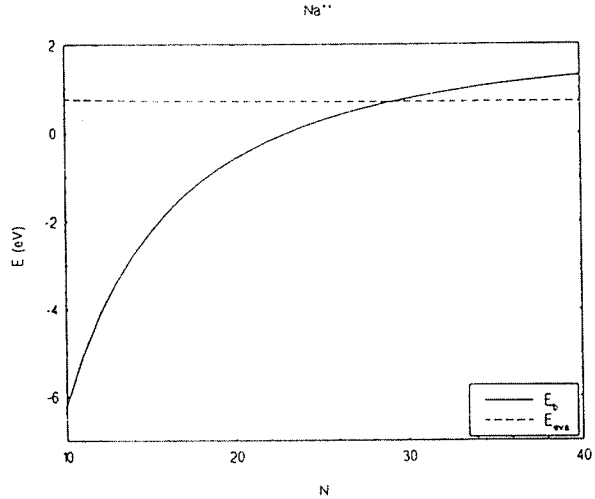

Figure 7: Lowest barrier height in comparison with the evaporation energy, both within the LDM.

together with the evaporation energy (by "most favored" we mean here the channel with the lowest barrier and not that with the lowest Q-value). The fission barrier increases with N, while the evaporation energy is practically constant. The two curves intersect at $N_c = 29$, in good agreement with the experimental number 27 [31]. But shell corrections should have an effect on N_c which remains to be investigated.

4. Conclusions

Nuclear Physics techniques and concepts are being applied to a new and exciting field of Physics. In contrast with Nuclear Physics, in Cluster Physics the exact force is known and systems with any size and charge can be considered.

Notwithstanding the differences in the structure and energy scale, the fission of metallic clusters display similarities with the fission of atomic nuclei. In both cases, fission is determined by the competition between the surface and Coulomb terms. However, the Coulomb term in atomic clusters arises from the surface charge, while in nuclei it is due to the volume charge. Fission occurs for small multiply charged clusters, whose surface tension is unable to sustain the surface Coulomb repulsion.

Shell effects play a major role in shaping fission barriers, changing drastically the liquid drop scenario. We have presented a method to evaluate potential energies of fragmentation processes which is simple but incorporates shell effects with an accuracy which is good enough for many practical purposes.

Acknowledgments

C. F. would like to acknowledge the kind invitation of A. Raduta to present this work at the Predeal school. We are grateful to M. Brajczewska (Coimbra), M. Brack (Regensburg), M. Seidl and J. P. Perdew (New Orleans) for fruitful discussions. This work has been partially supported by the EC- Science project "Study of the stability of charged metal clusters".

References

1. W. D. Knight, K. Klemenger, W. A. De Heer, W. A. Saunders, M. Y. Chou, and M. L. Cohen, *Phys. Rev. Lett.* **52** (1984) 2141.
2. W. Ekardt, *Phys. Rev.* **B31** (1985) 6360.
3. P. Hohenberg and W. Kohn, *Phys. Rev.* **136** (1964) B864.
4. W. Kohn and L. J. Sham, *Phys. Rev.* **140** (1965) A1133.
5. M. Brack, *Rev. Mod. Phys.* **65** (1993) 677.
6. J. P. Perdew, in *Density Functional Theory*, ed. E. K. U. Gross and R. M. Dreizler (Plenum, New York, 1994).
7. J. P. Perdew and Y. Wang, *Phys. Rev.* **B45** (1992) 13244.
8. M. Brack, C. Guet, and H.-B. Hakansson, *Phys. Rep.* **123** (1993) 275.
9. C. Fiolhais and J. P. Perdew, *Phys. Rev.* **B45** (1992) 6207.
10. N. D. Lang and W. Kohn, *Phys. Rev.* **B1** (1970) 4555.

11. J. P. Perdew, in *Condensed Matter Theories*, vol. IV, ed. J. Keller (Plenum, New York, 1989).
12. M. Seidl and M. Brack, *Ann. Phys. (N. Y.)*, in print.
13. E. Engel and J. P. Perdew, *Phys. Rev.* **B43** (1991) 1331.
14. J. P. Perdew, P. Ziesche, and C. Fiolhais, *Phys. Rev.* **B47** (1993) 16460.
15. P. Ziesche, J. P. Perdew, and C. Fiolhais, *Phys. Rev.* **B49** (1994) 7916.
16. J. P. Perdew, Y. Wang, and E. Engel, *Phys. Rev. Lett.* **66** (1991) 508.
17. M. Durand, P. Schuck, and X. Viñas, *Z. Phys.* **A346** (1993) 87.
18. V. M. Strutinsky, *Nucl. Phys.* **A95** (1967) 420.
19. V. M. Strutinsky, *Nucl. Phys.* **A122** (1968) 1.
20. J. R. Nix, *Ann. Rev. Nucl. Sci.* **22** (1972) 65.
21. U. Näher, H. Goehlich, T. Lange, and T. P. Martin, *Phys. Rev.* **B68** (1992) 3416.
22. M. P. Iñiguez, J. A. Alonso, M. A. Aller, and L. C. Balbás, *Phys. Rev.* **B34** (1986) 2152.
23. A. Vieira, M. Brajczewska, and C. Fiolhais, *Int. J. Quantum Chem.*, in print.
24. C. Bréchignac, Ph. Cahuzac, F. Carlier, and M. de Frutos, *J. Chem. Phys.* **93** (1990) 7749.
25. A. Vieira and C. Fiolhais, unpublished.
26. P. Holzer, U. Mosel, and W. Greiner, *Nucl. Phys.* **A138** (1969) 241.
27. D. Scharnweber, W. Greiner, and U. Mosel, *Nucl. Phys.* **A164** (1971) 257.
28. H. Koizumi, S. Sugano, and Y. Ishii, *Z. Phys.* **D28** (1993) 223.
29. J. Blocki, *Journal de Physique* **45 C6** (1984) 489.
30. R. N. Barnett, U. Landman, and G. Rajagopal, *Phys. Rev. Lett.* **67** (1991) 3058.
31. C. Bréchignac, Ph. Cahuzac, F. Carlier, and M. de Frutos, *Phys. Rev. Lett.* **64** (1990) 2893.